

Perturbation evolution with a non-minimally coupled scalar field

Rachel Bean,
Theoretical Physics, The Blackett Laboratory,
Imperial College, Prince Consort Rd.,
London SW7 2BZ
(28th April 2001)

We recently proposed a simple dilaton-derived quintessence model in which the scalar field was non-minimally coupled to cold dark matter, but not to ‘visible’ matter. Such couplings can be attributed to the dilaton in the low energy limit of string theory, beyond tree level. In this paper we discuss the implications of such a model on structure formation, looking at its impact on matter perturbations and CMB anisotropies. We find that the model only deviates from Λ CDM and minimally coupled theories at late times, and is well fitted to current observational data. The signature left by the coupling, when it breaks degeneracy at late times, presents a valuable opportunity to constrain non-minimal couplings given the wealth of new observational data promised in the near future.

Key words: Cosmology: theory.

I. INTRODUCTION

There is recent evidence ([1]- [3]) that the Universe’s expansion is accelerating. If this is so, it would have fundamental cosmological implications, for progressing the dark matter problem and reconciling a high Hubble Constant, $h \sim 0.65$, with an old Universe $t_0 > 11Gyr$. To explain such an acceleration, the Universe would have to have a matter component, additional to ordinary matter and radiation, since the latter two have equations of state that are unable to generate the required kinematics. In line with current observational constraints, the additional matter would have to have an equation of state $p = w\rho$ with $w \in (-1, -0.4)$ ([4]- [6]).

A pure cosmological constant cannot explain the observed acceleration without running into fine tuning problems; one would need $\Lambda \sim 10^{-122}c^3/(\hbar G)$, several hundreds of orders of magnitude lower than one would expect from a vacuum energy originating at the Planck time [7]. This has led to a wealth of proposals using a scalar “quintessence” field, minimally coupled to matter through gravity, which can be cajoled into acting as an effective cosmological constant in the presence of a suitable potential. Models of particular interest use “tracker” potentials (e.g. [8]- [13]) which allow the scalar field to produce the required dynamics without dependence on initial conditions, but these still require small-scale parameters. More recently, a model was proposed ([14], [15]) with a potential whose parameters were, a more physically agreeable, Planck scale. Explaining why the acceleration has only arisen recently, however, still requires some degree of fine-tuning in the model parameters, if not in the initial conditions, in order to confine acceleration to the current epoch [16]. A more practical explanation for the coincidental acceleration nowadays is that we are in close proximity to the cosmological transition from radiation to dust domination. Armendariz-Picon, Mukhanov and Steinhardt [17] utilised this proxim-

ity to drive the dynamics of their κ -essence model although the Lagrangian used is somewhat complex, consisting of a series of non-linear kinetic terms.

In a recent paper [18], we proposed a simpler model which harnesses the dynamical shift in the radiation-dust transition using a non-minimally coupled scalar field. We showed that a coupling of this form can use the transition to dust domination to push a quintessence field off scaling behaviour, and produce acceleration in the background nowadays.

In this paper we consider the impact of such a non-minimal coupling on the evolution of perturbations to the background and the subsequent implications for both structure formation and the Cosmic Microwave Background (CMB).

We start by giving an overview of the coupled quintessence model, and then go on to discuss the implications of coupling for perturbation evolution and structure formation.

II. COUPLED QUINTESSENCE MODEL

Non-minimal theories are commonly expressed in one of two frames. In one, the problem is posed in the Jordan frame and the scalar field is directly coupled to curvature, in the form $f(\phi)\mathcal{R}$, and produces a departure from Einstein’s gravity, as is seen in Brans-Dicke theories [19]. This effect was used by [20] to force the quintessence field out of scaling behaviour, necessary to give accelerated dynamics, however this “R-boost” occurs early in the radiation epoch and cannot explain acceleration today. In the second, the Einstein frame is used and the scalar field instead couples to terms in the matter Lagrangian resulting in dynamical, field-dependent, masses and polarisations. These two groups are interrelated through conformal transformation of the metric; any theory in one frame can be rephrased in the other. However, usually a simple function in one frame is mapped into a compli-

cated function in the other. Such couplings are heavily constrained when applied to the visible matter in the Universe, whether to photons [21], or to what is usually called baryons [22]. However, it could be that the dilaton coupled differently to visible matter and to the dark matter of the Universe. This hypothesis was suggested in [23], and allows for large couplings to be consistent with observations (see also [24], [25]). We consider a scenario in which such a case exists.

We choose $g^{\mu\nu}$ to have convention (+ - -) in a flat FRW background. All quantities are expressed in units with $M_P = (8\pi G_N)^{-1/2} = 1$ where M_P is the Planck mass and G_N is the Newtonian Gravitational constant. We consider a Lagrangian of the form:

$$\mathcal{L} = \sqrt{-g} \left(-\frac{R}{2} + \frac{1}{2} \partial_\mu \phi \partial^\mu \phi - V(\phi) + \mathcal{L}_V + f(\phi) \mathcal{L}_c \right) \quad (1)$$

in which \mathcal{L}_V is the Lagrangian of “visible matter” (baryons, photons, and also baryonic and neutrino dark matter), and \mathcal{L}_c the Lagrangian of a dominant non-baryonic form of cold dark matter. We take $V(\phi) = V_0 e^{-\lambda\phi}$ the standard quintessence potential, which drives scaling behaviour when the coupling is minimal ([11], [12]).

The coupling investigated is of the form $f(\phi) = 1 + \alpha(\phi - \phi_0)^\beta$. Couplings of this form could arise as generalisations of an effective action for massless modes of a dilaton [22] after performing a conformal transformation from the string frame into the Einstein frame. α and β are parameters reflecting the shape of the minimum being approached by the coupling [26].

A. Background Evolution

Here we discuss the background equations in the conformal FRW metric, which are derived in appendix VIA. The field equations are obtained by varying the action with respect to the metric and the scalar field:

$$G_{\mu\nu} = T_{\mu\nu}^{(V)} + T_{\mu\nu}^{(\phi)} + f(\phi) T_{\mu\nu}^{(c)} \quad (2)$$

$$\nabla^2 \phi = \frac{\partial V}{\partial \phi} - \frac{\partial f}{\partial \phi} \mathcal{L}_c \quad (3)$$

where $G_{\mu\nu}$ is the Einstein’s tensor and the various $T_{\mu\nu}$ are stress-energy tensors. Heuristically, we may interpret the new term driving ϕ as a contribution to an effective potential $V_{eff} = V - f(\phi) \mathcal{L}_c$. Bianchi’s identity ($\nabla_\mu G_\mu^\nu = 0$) leads to :

$$\nabla_\nu T^{\mu\nu(V)} = 0 \quad (4)$$

$$\nabla_\nu T^{\mu\nu(c)} = (g^{\mu\nu} \mathcal{L}_c - T_c^{\mu\nu}) \frac{f'}{f} \nabla_\nu \phi \quad (5)$$

These are to be contrasted with Amendola’s coupled quintessence [27] (for which the interaction term is proportional to T).

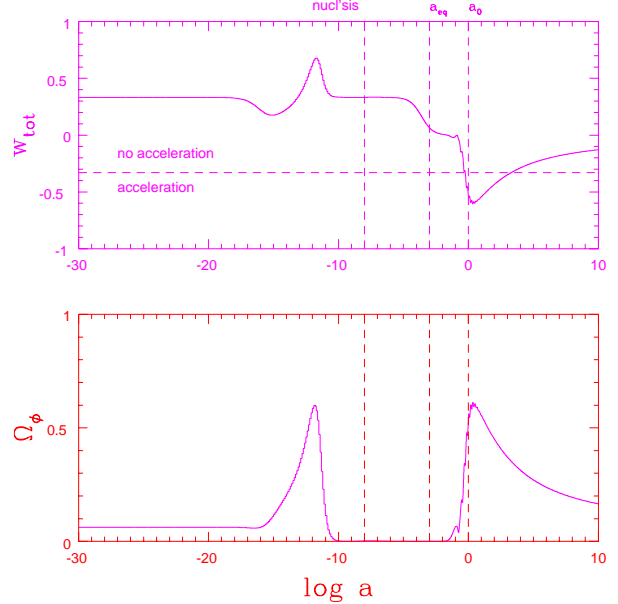


FIG. 1. The evolution of Ω_ϕ and w_{tot} for a model with $\lambda = 8$, $\beta = 8$, $\alpha = 50$, and $\phi_0 = 32.5$ (and $\Omega_b = 0.053$, $h = 0.65$). An early period of scaling is broken near the transition from radiation to matter, first with a period of kination, then inflation. At late times the universe returns to a matter dominated scaling solution.

Evaluating the components of the field equations, with scale factor a , we find Friedmann equations:

$$\frac{3}{a^2} \left(\frac{\dot{a}}{a} \right)^2 = \rho_b + \rho_\gamma + f(\phi) \rho_c + \frac{1}{2} \dot{\phi}^2 + V(\phi) \quad (6)$$

$$\dot{\rho}_c + 3 \frac{\dot{a}}{a} \rho_c = -\frac{f'(\phi) \dot{\phi}}{f(\phi)} (\rho_c + \mathcal{L}_c) = 0 \quad (7)$$

$$\rho_b + 3 \frac{\dot{a}}{a} \rho_b = 0 \quad (8)$$

$$\rho_\gamma + 4 \frac{\dot{a}}{a} \rho_\gamma = 0 \quad (9)$$

$$\ddot{\phi} + 2 \frac{\dot{a}}{a} \dot{\phi} + a^2 V' = f'(\phi) \mathcal{L}_c a^2 = -f'(\phi) \rho_c a^2 \quad (10)$$

where dots represent derivatives with respect to conformal time, and the prime (') indicates differentiation with respect to ϕ .

One notices in equation (7) that the evolution of the background coupled dark matter is unaffected by the coupling. This simply arises because we are coupling to pressureless matter for which $\mathcal{L}_c = -\rho_c$; if we had instead coupled to radiation we would find $\mathcal{L}_c = 0$ and the coupling would have altered the background evolution (as discussed in appendix VIA). However as will be discussed later, observations measure the coupled energy density $f(\phi) \rho_c$ not simply ρ_c so that the magnitude of the observed matter is affected by the coupling through (10).

Fig.1. shows the evolution of Ω_ϕ and overall equa-

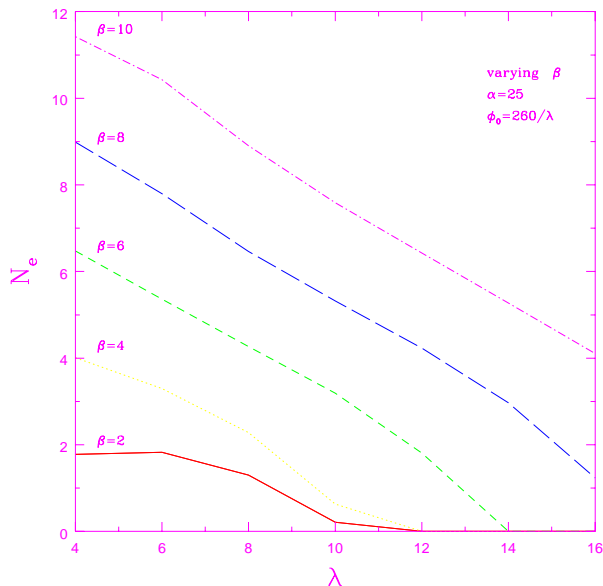


FIG. 2. The amount of accelerated expansion produced with the model for various values of β , measured in the number of e-foldings $N_e = a_f/a_i$. a_i and a_f are the expansion scales when inflation begins and ends, respectively, ($a_i < a_0 \leq a_f$, where $a_0 = 1$ is the expansion scale nowadays). We have given $\alpha = 25$ as an example with $\phi_0 = 260/\lambda$.

tion of state $w_{tot} = \rho_{tot}/p_{tot}$ for one model scenario. One can see that deep in the radiation epoch the coupling has a negligible effect on the overall dynamics and the scalar field's energy density scales with that of the dominant radiation, as in the minimally-coupled case. As the transition from radiation to matter domination is approached the coupling becomes important and the dynamics are driven away from scaling behaviour. The driving term on the right hand side of equation (10) first, transiently, drives the field to kinetic, suppressing the evolution of the scalar field and $\Omega_\phi \sim 0$, then it re-emerges into inflationary behaviour to provide the accelerated expansion we observe today. The model requires that β be even and that the value of ϕ_0 is of the order of magnitude of the scalar field today. However given these constraints, the model provides acceleration for a wide range of parameters as shown in the parameter space plots for the non-minimally coupled model in Figs. 2 and 3.

In minimally coupled models with exponential potentials, the value of the parameter λ is limited by BBN constraints [28] to be $\lambda \geq 8$ however the NMC model avoids this constraint through the suppression of Ω_ϕ at nucleosynthesis, irrespective of λ 's value. Parameter constraints for the non-minimal case can only therefore come from CMB and matter power spectrum predictions discussed below. In order to compare the non-minimal models with analogous minimally coupled ones however, we consider cases with $\lambda = 8$ in

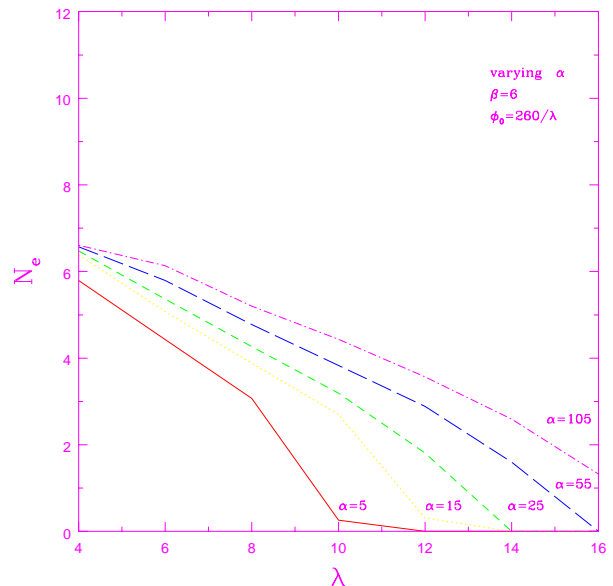


FIG. 3. The amount of accelerated expansion produced with the model as α is varied, measured again in the number of e-foldings N_e . We have given $\beta = 6$ as an example with $\phi_0 = 260/\lambda$.

our discussion below.

B. Observational implications

It is pertinent to consider whether the effect of the non-minimal coupling on the background at late times could be seen in current observations, i.e. when looking at the predicted apparent magnitude versus redshift relation at $z < 2$.

The apparent bolometric magnitude is given by

$$m(z) = M + 5 \log d_L(z) + 25 \quad (11)$$

where M is the absolute bolometric magnitude, and d_L is the luminosity distance in Mpc

$$d_L = (1+z) \int_0^z \frac{dz'}{H(z')} \quad (12)$$

In Fig.4 we plot the effective bolometric magnitude from the B-band filter, $m_B^{eff}(z)$, from the Calán Tololo [29] and SCP [6] surveys and predicted $m(z)$ curves for the non-minimally coupled model in Fig.1 and a comparative Λ CDM model. The effective magnitude is obtained from the apparent magnitude after taking into account the lightcurve width-luminosity correction, galactic extinction and the K-correction from the differences in the observed R-band and restframe B-band filters [6]. Within current observational error constraints, the non-minimally coupled model cannot be distinguished from the Λ CDM model. Recently

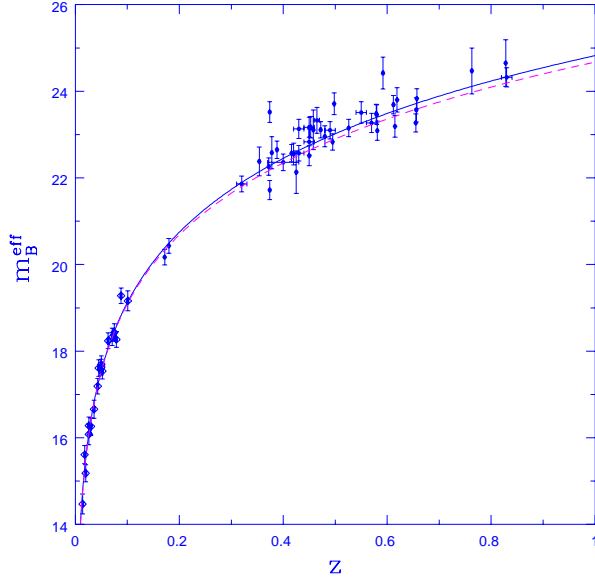


FIG. 4. Plot of the effective bolometric magnitude for the Calán Tololo (open diamonds) and SCP data points (solid circles) against redshift. The curves correspond to two models considered in this paper Λ CDM model (solid line) with $\Omega_c = 0.347, \Omega_b = 0.053$ and $\Omega_\Lambda = 0.6$ and a non-minimally coupled model with $f(\phi)\Omega_c = 0.347, \Omega_b = 0.053$ and $\Omega_\phi = 0.6$ with model parameters specified in Fig.1.

proposed observational projects (see for example [30]) may offer future hope to discriminate between the effect of quintessence models on the background evolution.

In the remainder of the paper, we consider an alternative approach to distinguishing between quintessence models, through their effect not on the background but on the perturbations about it.

III. IMPLICATIONS FOR STRUCTURE FORMATION

The addition of the scalar field has implications for structure formation both due to the addition to the homogeneous background energy density, and secondly by the generation and evolution of scalar field perturbations. The additional background energy density shifts the equality redshift and alters the angular distance to the last scattering surface. The scalar field also introduces extra terms in the perturbed Einstein equations and opens up the possibility of isocurvature perturbations evolving.

We study the impact of these effects by calculating the linear perturbation equations and specifying the initial conditions. These are then evolved from early on in the radiation epoch when the coupling is unimportant through to nowadays. The matter and CMB

power spectra are then calculated and compared with those obtained with minimally coupled models and observations.

A. Linear perturbation evolution

We follow the approach and notation of Ma and Bertschinger [31] extended by Ferreira and Joyce [12] for minimally coupled scalar fields. A simplified model containing no baryons is used for the discussion, although a full theory containing baryons and relativistic neutrinos is used to obtain the CMB and matter power spectrum predictions presented. The essential results are presented here, while a full derivation of the equations can be found in the appendix VI B.

Consider perturbations to a flat FRW metric in the synchronous gauge, with line element

$$ds^2 = a(\tau)^2 \{-d\tau^2 + (\delta_{ij} + h_{ij})dx^i dx^j\} \quad (13)$$

We will only be concerned with the scalar modes of the perturbation, for which we can parameterise the metric perturbation as

$$h_{ij} = \int d^3k e^{ik \cdot x} [\hat{k}_i \hat{k}_j h(k, \tau) + (\hat{k}_i \hat{k}_j - \frac{1}{3} \delta_{ij} 6\eta(k, \tau))] \quad (14)$$

where h is the trace of the metric perturbation. To obtain the linear perturbation evolution equations we consider the perturbed Einstein equations

$$k^2 \eta - \frac{1}{2} H \dot{h} = 4\pi G a^2 \delta T_0^0 \quad (15)$$

$$k^2 \dot{\eta} = 4\pi G a^2 i k_i \delta T_i^0 \quad (16)$$

$$\ddot{h} + 2H \dot{h} - 2k^2 \eta = -8\pi G a^2 \delta T_i^i \quad (17)$$

$$\ddot{h} + 6\dot{\eta} + 2H(\dot{h} + 6\dot{\eta}) - 2k^2 \eta = 24\pi G a^2 (\hat{k}_i \hat{k}_j - \frac{1}{3} \delta_{ij}) \Sigma_j^i \quad (18)$$

where Σ_j^i is the traceless shear. Writing the perturbations to energy densities, ρ , pressures, p , and the scalar field, in terms of a homogeneous background plus a perturbation, we have

$$\rho(x, \tau) = \rho(\tau)(1 + \delta(x, \tau)) \quad (19)$$

$$p(x, \tau) = p(\tau) + \delta p(x, \tau) \quad (20)$$

$$\Phi(x, \tau) = \phi(\tau) + \varphi(x, \tau) \quad (21)$$

The only perturbation in T_ν^μ to be affected by the coupling is δT_0^0 , the other perturbations are the same as for a minimally coupled model,

$$\delta T_0^0 = -\rho_\gamma \delta_\gamma - (\varphi f' + f \delta_c) \rho_c - \left(\frac{1}{a^2} \dot{\varphi} \dot{\phi} + \varphi V'\right) \quad (22)$$

$$i k_i \delta T_i^0 = \frac{4}{3} \rho_\gamma \theta_\gamma + \frac{1}{a^2} \dot{\phi} \nabla^2 \varphi \quad (23)$$

$$\delta T_i^i = 3 \left(\frac{1}{3} \rho_\gamma \delta_\gamma + \frac{1}{a^2} \dot{\varphi} \dot{\phi} - \varphi V' \right) \quad (24)$$

where θ is the velocity divergence. The evolution equations of the density perturbations for radiation and the dark matter component are the final requirement. One finds, as is shown in VIB, that the coupling does not effect the first order equation for the matter perturbation so that,

$$\delta_\gamma = -\frac{4}{3}\theta_\gamma - \frac{2}{3}\dot{h} \quad (25)$$

$$\delta_c = -\theta_c - \frac{1}{2}\dot{h} \quad (26)$$

The spare degree of freedom in the synchronous gauge allows us to choose the background, synchronous coordinates. As is conventional, we do this by constraining the dark matter field such that $\theta_c = 0$, which fixes $\delta_c = -\frac{1}{2}\dot{h}$. We are now able to write down the perturbation equations for the non-minimally coupled system.

$$\begin{aligned} \ddot{\delta}_c + H\dot{\delta}_c + \frac{3H^2\Omega_c f}{2}\delta_c \\ = -3H^2\Omega_\gamma\delta_\gamma - 2\dot{\varphi}\dot{\phi} + (a^2V' - \frac{3H^2\Omega_c f'}{2})\varphi \end{aligned} \quad (27)$$

$$\begin{aligned} \ddot{\varphi} + 2H\dot{\varphi} + [k^2 + a^2(V'' + f''\rho_c)]\varphi \\ = -\frac{1}{2}\dot{h}\dot{\phi} - a^2f'\rho_c\delta_c \end{aligned} \quad (28)$$

$$\ddot{\delta}_\gamma - \frac{k^2}{3}\delta_\gamma = \frac{4}{3}\ddot{\delta}_c \quad (29)$$

The non-minimal coupling introduces extra terms into the equations for matter and scalar field perturbations, altering the mass terms and source terms, the latter shown on the right hand side of the equality for clarity. The coupling will only affect the radiation perturbations indirectly through the background bulk (via H) and through $\dot{\delta}_c$.

Deep in the radiation epoch, the coupling to dark matter is unimportant. The adiabatic perturbation evolution closely follows the power-law solutions for the minimally coupled model with an exponential potential as discussed by Ferreira and Joyce [12]. The growing modes of δ_γ, δ_c and φ evolve $\propto \tau^2$

$$\begin{aligned} \delta_\gamma = -\frac{2}{3}C(k\tau)^2, \quad \delta_c = -\frac{1}{2}h = \frac{3}{4}\delta_\gamma, \\ \varphi = -\frac{2}{5\lambda}h, \quad \dot{\varphi} = -\frac{2}{5\lambda}\dot{h} \end{aligned} \quad (30)$$

where C is an arbitrary normalisation constant.

It's only at very late times, $z \lesssim 2$, that the coupled matter establishes itself as the dominant effect on growth. This is when we would expect the coupling's signature to start to be seen.

So far only pure curvature (adiabatic) perturbations have been considered, however isocurvature perturbations might also exist in quintessence models [32]. For this non-minimal model we believe that their impact is negligibly small. Isocurvature perturbations are known to be negligible in minimally coupled tracking quintessence models. This will also be so for

the non-minimally coupled case early on in the radiation epoch, where the couplings effect is unimportant. When the field is driven off tracking, close to the transition from matter to radiation, we cannot assume this, however. During the period when tracking is broken, the scalar field is suppressed and $\Omega_\phi \sim 0$ (see fig.1). In general, the non-adiabatic pressure perturbation δp_{non-ad} is given by

$$\frac{\delta p_{non-ad}}{\rho + p} = \mathcal{O}(\Omega_\phi)(\delta_\gamma + \delta_\phi) \quad (31)$$

Therefore, since the quintessence contribution to the total energy density is highly suppressed, the isocurvature contributions will continue to be small away from tracking behaviour, around the transition time. It is only at very late times, after last scattering, when Ω_ϕ is no longer small, that the isocurvature perturbations may start to grow. For the following discussion, therefore, we only consider adiabatic perturbations.

B. Implications for matter perturbations

An important consequence of non-minimal coupling is that, when considering the coupled matter, it is the *coupled energy density*, $f\rho_c$, that should be interpreted as the matter density measured in observations, not ρ_c ; an analogous case is non-minimally coupled gravity, $f(\phi)\mathcal{R}$, in which we consider the varying gravitational field strength as the observable and not constant Newtonian gravity, G_N . So we are interested in the effective dark matter density $\tilde{\delta}_c$

$$\tilde{\delta}_c = \frac{\delta(f\rho_c)}{f\rho_c} = \delta_c + \frac{f'}{f}\varphi \quad (32)$$

An insightful way to look at the coupling's effect on perturbation growth is by looking at its effect on the dimensionless growth rate

$$n_{eff} = \tau \frac{\dot{\tilde{\delta}}_c}{\tilde{\delta}_c} \quad (33)$$

In Fig. 5 the growth rate for one scale, $k = 0.1Mpc^{-1}$, is shown for various models, in each case $h=0.65$, $\Omega_b=0.053$. A non-minimally coupled (NMC) model with $\Omega_\phi = 0.6$ and $\lambda = 8(\beta = 8, \phi_0 = 32.5)$, is compared with a Λ CDM model, $\Omega_\Lambda = 0.6$, a sCDM model $\Omega_c = 0.947$, and an analogous minimally coupled (MC) quintessence model using the potential developed by Albrecht and Skordis [14] $V = V_0 e^{-\lambda\phi}(A + (\phi - \phi_0)^B)$ with $\lambda = 8$ ($A=0.01, B=2, \phi_0 = 32.5$). For $z > 2$ the growth rates for the scalar field models do not differ greatly from that in the Λ CDM model.

The addition of a scalar field or cosmological constant, with $\Omega_0 = 1$ fixed, will act to reduce Ω_c and therefore the size of the mass term in equation (27). This is the main factor responsible for the suppression of growth at later times, rather than the non-clumping behaviour of the scalar field commonly cited

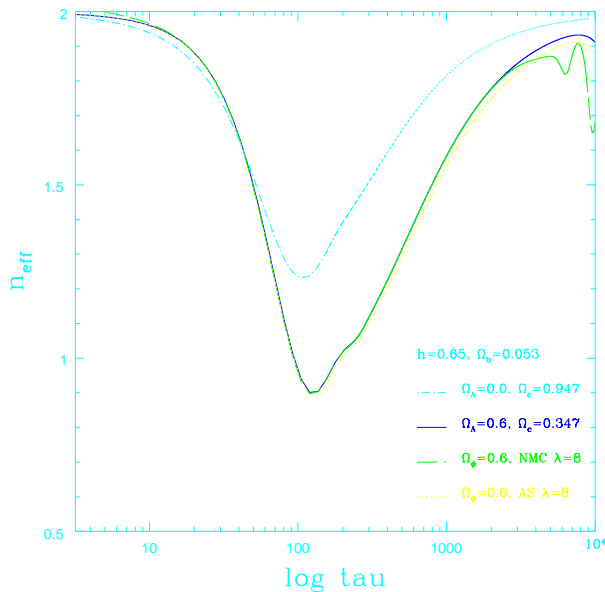


FIG. 5. Time evolution of the effective growth rate for 4 scenarios (all $h=0.65$, $\Omega_b = 0.053$), 3 of which produce acceleration today: 1) Λ CDM $\Omega_\Lambda = 0.6$ (full line), 2) NMC model $\Omega_\phi = 0.6$, $\lambda = 8$, $\beta = 8$, $\phi_0 = 32.5$ (long dash), 3) MC model $\Omega_\phi = 0.6$, $\lambda = 8$, $A = 0.01$, $B = 2$, $\phi_0 = 32.5$ (short dash), and one which doesn't: 4) sCDM model $\Omega_c=0.947$ (dot-dash)

as the cause. Sub-horizon scalar field perturbations have oscillatory time evolution with decaying amplitudes, their contribution to the evolution of matter perturbations therefore is small for the observationally interesting scales. For NMC models, the coupling suppresses Ω_ϕ around z_{eq} , making the scalar field contribution to δ_c growth negligible. Subsequently, the growth rate for NMC models is closer to that created by a cosmological constant than for the MC models.

At late times however, for $z < 2$, the coupling and scalar field become important, and act to suppress the growth in δ_c to a far greater extent than Λ and MC models, offering a potential way to distinguish non-minimal from minimal the NMC model.

The dampening effect can be also seen in the matter power spectrum $P(k)$,

$$P(k) = \langle |\tilde{\delta}_c(k)|^2 \rangle = (100C)8\pi^3 h^3 k \left(\frac{k}{k_0} \right)^{n-1} \quad (34)$$

where C is the normalisation factor from CMBFAST [33] arising from the Bunn & White normalisation [34] at $l=10$ multipole, k is in units of h/Mpc and $k_0 = 0.05 \text{Mpc}^{-1}$ and n is the tilt, chosen here $n=1$ for a scale invariant spectrum.

In fig 6. the matter power spectra for the both the NMC and MC models mimic a Λ CDM model for scales $k < \sim 0.1$ i.e. those modes having entered the horizon before and around equality. There is a slight suppres-

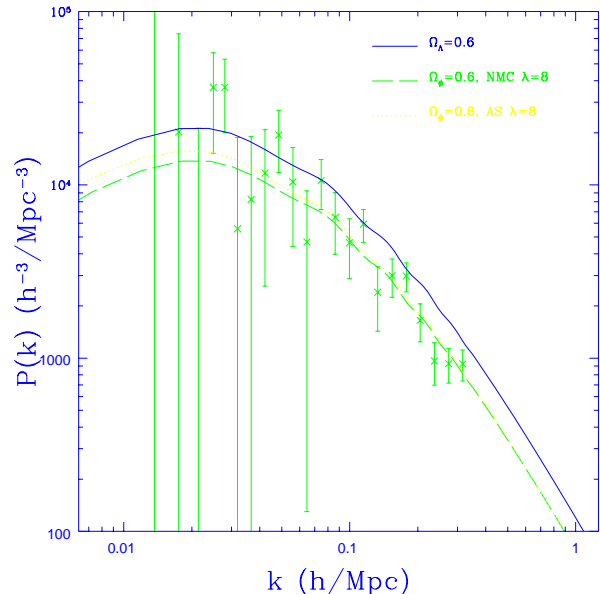


FIG. 6. Matter power spectrum for the 3 scenarios in Fig. 5 which produce acceleration today: Λ CDM (full), NMC (long dash) and MC (short dash), together with the de-correlated data points of Hamilton et al. Parameters in the 3 models are the same as in Fig.5.

sion but a bias factor could in theory resolve the discrepancy. Certainly all three models give reasonable predictions for matter fluctuations over a sphere of size $8h^{-1}\text{Mpc}$ with $\sigma_8 = 0.89, 0.91, 1.13$ for NMC, MC and Λ CDM models respectively, in comparison to the observed value $\sigma_8 = 0.56\Omega_m^{-0.47} \sim 0.9$ [35].

For larger scales, however, the coupling does make a difference. In scales that have only entered the horizon in recent times, whilst the coupling is important, we see a distinctive reduction of power in comparison to the MC and Λ CDM models which tend to similar behaviour. Although the suppression clearly distinguishes the coupled model, its profile is still consistent with current observational results [36]. There may be an opportunity with the future SLOAN galaxy survey results to constrain the power spectrum at these larger scales (to $k \sim 0.01$).

Another potential impact of the late time importance of the coupling is that it will affect small scale features at $z \sim 2$, observable potentially through future weak lensing (see e.g. [37] and references therein) and damped Lyman α cloud measurements (see e.g [38]).

C. Impact on CMB anisotropies

Introducing a scalar field can potentially have several effects on the CMB power spectrum. Firstly, as we have already mentioned in section III A, the scalar

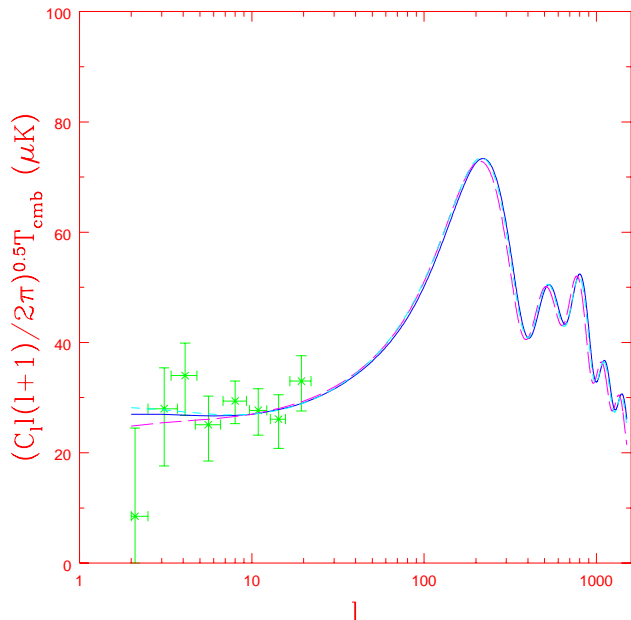


FIG. 7. CMB power spectra showing low l (plateau) behaviour for the 3 scenarios in Fig. 5: Λ CDM (full), NMC (long dash) and MC (short dash) with COBE datapoints. Model parameters are the same as in Fig. 5. The 3 models evolve differently at late times producing slightly different ISW anisotropies shown in the plateau at low l . However observations at this scale are dominated by cosmic variance, so that the differences would not be observable.

field gives rise to extra mass and source terms in the linear evolution equations for φ and δ_c . These then indirectly affect the radiation perturbations, altering the acoustic peak positions and heights at the time of last scattering (τ_{lss}). However, the scalar perturbations are effectively negligible around z_{eq} , especially in the NMC scenario so this effect will be minimal.

Secondly, the time varying Newtonian potential after decoupling will be affected by the coupling, altering the anisotropies produced at large angular scales (the Integrated Sachs-Wolfe effect). This can be seen in fig. 7 where the NMC model has a different profile at small l from the MC and Λ CDM models. However the effect is not large enough to be disentangled from the effect of cosmic variance.

Thirdly, the inclusion of the scalar field alters the composition of the energy density, altering the angular diameter distance of the acoustic horizon size at recombination. This can be parameterised by the value of \mathcal{B}

$$\mathcal{B} = \Omega_c^{1/2} h \int_{z_{rec}}^{z_0} dz \left\{ \sum \Omega_j z^{3(1+w_j)} \right\}^{-1/2} \quad (35)$$

Altering the value of \mathcal{B} shifts the positions of the peaks. The critical problem one confronts when trying to use CMB spectra to differentiate between models is the degeneracy that exists between models with

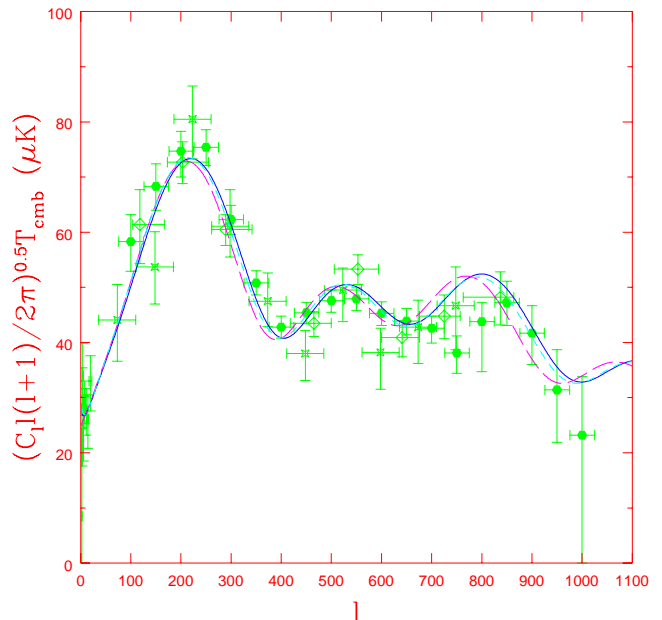


FIG. 8. CMB power spectra showing acoustic peaks for the 3 scenarios in fig.5: Λ CDM (full), NMC (dash) and MC (short dash), together with the data from Boomerang (solid circles), Maxima (crosses) and DASI (open diamonds). Model parameters are the same as in Fig. 5.

identical Ω_c, Ω_b and \mathcal{B} [39]. It has been shown that this degeneracy can be broken for scalar field models in which a large fraction of the energy density at τ_{lss} is from the scalar [28]; the scalar field acting as an effective increase in the number of relativistic degrees of freedom. However for models in which $\lambda \geq 8$ the degeneracy still exists in minimally coupled models. In Figs. 7 and 8, CMB spectra are plotted for the scenarios discussed in the previous section against COBE [40], MAXIMA [41], Boomerang [42] and DASI [43] data. All the models discussed have $\mathcal{B}=1.77$ and yet one can see that the degeneracy of the first peak is slightly broken, with the NMC model having $l_{peak}=215$ in comparison to 224 for both the MC and Λ CDM models. It is also interesting to note that the CMB spectra for coupled models with different λ values are effectively degenerate in themselves, as shown in the figure. This implies that, although coupling itself may be distinctive, CMB spectra will not be able to isolate the parameter in the potential.

The fourth possible effect is on the separation of the peaks. This has been proposed as a possible mechanism with which to distinguish minimally coupled models [44]. They are not distinguishable from Λ CDM if $\Omega_\phi(\tau_{lss})$ is small however, as mentioned above. But in the case of non-minimally coupled models the degeneracy in the second and third peaks is broken because of the effect the coupling has on τ_0 the conformal time nowadays. This is of particular interest

given the expected improvements in peak definition (e.g [42], [41], [43], [45]). The separation of the peaks dl is given by

$$\delta l = \pi \frac{\tau_0 - \tau_{lss}}{r_s} \quad (36)$$

where r_s is the sound horizon and c_s , the baryon speed of sound, both of which can be assumed effectively constant across the models. The NMC model has $\tau_0=12,530$ in comparison to $\tau_0=13,077$ for the Λ CDM model. This reduces the separation slightly breaking the degeneracy, as shown; the separation of the first and second peaks in the NMC model is $dl=309$ in comparison to 327 Λ CDM scenario.

Although distinguishable from the cosmological constant spectrum, the difference is still too small to be resolved with current observational data, including the most recent Boomerang [42] and DASI [43] data, showing highly improved definition in the second and third peaks. However with a number of observational projects continuing to focus attention on resolving the higher peaks, the breaking of degeneracy may offer a way to constrain non-minimally coupled models. In Fig.9 we plot the residual differences between the Λ CDM and NMC C_l spectra in Fig.8 when compared with estimated MAP errors. The parameters used to estimate the MAP errors are shown in appendix VI C. The estimated errors are considerably smaller than these residual levels for $l < 900$ implying that we may be able to distinguish between these various models within the near future.

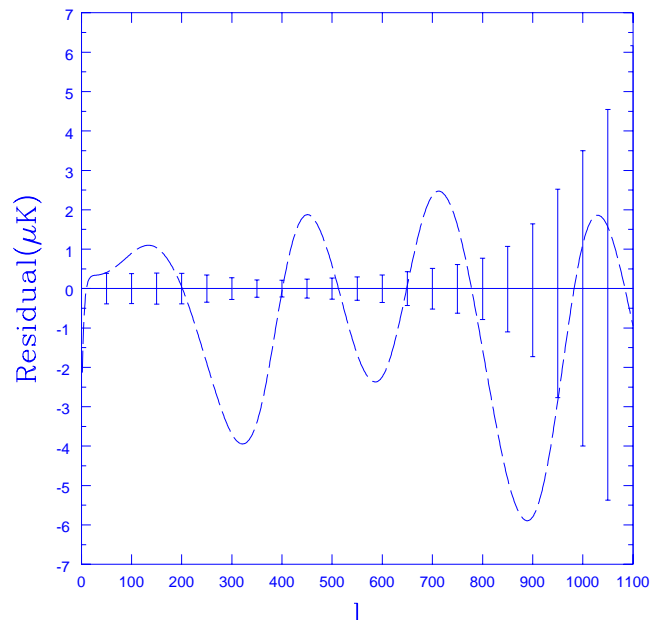


FIG. 9. Residual deviation of the the NMC model's temperature fluctuations from those of the Λ CDM model, both shown in Fig.8., with estimated MAP error bars.

IV. CONCLUSION

We have examined the impact a scalar field, non-minimally coupled to cold dark matter will have on the evolution of matter and radiation perturbations. We considered firstly its impact on the linear evolution equations and found that even though it did introduce new terms these were effectively negligible for all but very late times. The impact of this late time behaviour was then considered for matter perturbations where it was seen to create a suppression of growth at large scales. The coupling was also found to break the degeneracy usually seen in the CMB spectrum, slightly shifting the position of the first peak and reducing the separation between adjacent peaks. These two distinctive 'signatures' of the coupled dark energy model are not resolvable with current observations. However projects currently underway look to mapping both the matter power spectrum and CMB peaks with much improved accuracy. These may offer an opportunity to eventually distinguish between Λ CDM, minimally coupled and non-minimal coupled quintessence models in the near future.

V. ACKNOWLEDGEMENTS

I would like to thank João Magueijo and Carlo Contaldi for many helpful conversations. RB acknowledges the financial support from PPARC.

VI. APPENDIX

A. Bianchi's Identity

In this section we derive the equations of motion for the coupled dark matter and scalar fields explicitly from the action.

$$\mathcal{S} = \int \sqrt{-g} d^4x \left(-\frac{\mathcal{R}}{2} + \frac{1}{2} \phi_{,\mu} \phi^{,\mu} - V(\phi) + \mathcal{L}_V + f(\phi) \mathcal{L}_c \right) \quad (37)$$

Bianchi's identity reflects the symmetry of the Riemann tensor, the Einstein tensor being covariantly conserved,

$$(\mathcal{R}^{\mu\nu} - \frac{1}{2} g^{\mu\nu} \mathcal{R})_{;\nu} = (T^{\mu\nu(\phi)} + T^{\mu\nu(V)} + f(\phi) T^{\mu\nu(c)})_{;\nu} = 0 \quad (38)$$

Since visible matter is minimally coupled in the model we can immediately separate it out,

$$T^{\mu\nu(V)}_{;\nu} = 0 \quad (39)$$

Using the explicit definition of the energy momentum tensor in terms of their Lagrangian,

$$T_{;\nu}^{\mu\nu} = \left[\frac{2}{\sqrt{-g}} \left(\frac{\partial(\sqrt{-g}\mathcal{L})}{\partial g_{\mu\nu}} \right) \right]_{;\nu} \quad (40)$$

so the scalar field component of the Bianchi identity in terms of ϕ and its derivatives is

$$T_{;\nu}^{\mu\nu(\phi)} = \phi^{;\mu} (\phi_{;\nu}^{\nu} + \Gamma_{\alpha\nu}^{\nu} \phi^{;\alpha} + V'(\phi)) \quad (41)$$

The Euler-Lagrange equation, which is just the Klein Gordon equation, allows us to simplify this further

$$\phi_{;\alpha}^{\alpha} + \Gamma_{\alpha\beta}^{\beta} \phi^{;\alpha} + V'(\phi) = f'(\phi) \mathcal{L}_c \quad (42)$$

Combining these two expressions we obtain

$$T_{;\nu}^{\mu\nu(\phi)} = f'(\phi) \mathcal{L}_c g^{\mu\nu} \phi_{;\nu} \quad (43)$$

For the coupled matter then,

$$\left(f(\phi) T^{\mu\nu(c)} \right)_{;\nu} = f' \phi_{;\nu} T^{\mu\nu(c)} + f T_{;\nu}^{\mu\nu(c)} \quad (44)$$

Combining the results in equations (39) and (43), Bianchi's identity in (38) is given by

$$T_{;\nu}^{\mu\nu(c)} = \frac{f'}{f} \phi_{;\nu} \left(\mathcal{L}_c g^{\mu\nu} - T^{\mu\nu(c)} \right) \quad (45)$$

We can obtain an expression for the Lagrangian for perfect fluid by considering it to be a gas of particles with masses m_a and paths x_a^i [46]

$$\mathcal{L}_a(x) = -m_a \delta(x - x_a(t)) (-g_{\mu\nu} \dot{x}^\mu \dot{x}^\nu)^{\frac{1}{2}} \quad (46)$$

By noting that the length of the 4-velocity $(-g_{\mu\nu} \frac{dx^\mu}{d\lambda} \frac{dx^\nu}{d\lambda})^{\frac{1}{2}} = ds/d\lambda$ equals 1 for dust, this expression simplifies greatly. Averaging over particles in the gas rest frame we find $\mathcal{L}_c = -n \langle m/u^0 \rangle$ where n is the particle number density and $u^\mu = dx^\mu/d\lambda$ is the 4-velocity. For pressureless particles $u^\mu = \{1, 0, 0, 0\}$ therefore $\mathcal{L}_c = -\rho_c$.

We can also obtain an expression for the stress-energy tensor from the Lagrangian in an analogous way. Using the relationship between $T^{\mu\nu}$ and \mathcal{L} in (40) the stress-energy for a particle is given by

$$T_a^{\mu\nu} = m_a \frac{\delta(x - x_a(t))}{\sqrt{-g}} \dot{x}^\mu \dot{x}^\nu u^0 \quad (47)$$

On averaging over the particles the energy density is $\rho = \langle T^{00} \rangle = n \langle m u^0 \rangle$ and the pressure in the x -direction is given by $p = \langle T^{11} \rangle = n \langle m u^0 (v^1)^2 \rangle$ where $v^i = dx^i/dt = u^i/u^0$, for dust therefore $p_c = 0$. In addition, in the rest frame there is zero streaming velocity so that $\langle T^{0i} \rangle = n \langle m u^0 v^i \rangle = 0$.

In this paper we assume that the coupled matter is comprised of cold pressureless dust particles. Putting the expression for \mathcal{L}_c into (45), the background evolution equation for non-minimally coupled matter is identical to that in the minimally coupled case.

$$T_{;\nu}^{\mu\nu(c)} = \dot{\rho}_c + 3H\rho_c = 0 \quad (48)$$

B. Linear perturbation equations

We here derive the linear perturbation equations for the coupled cdm and scalar fields in detail. We assume the notation of Ma and Bertschinger [31] and results of Ferreira and Joyce [12]. Consider perturbations to a flat FRW metric in the synchronous gauge, with line element

$$ds^2 = a(\tau)^2 \{ -d\tau^2 + (\delta_{ij} + h_{ij}) dx^i dx^j \}$$

By considering the perturbed Euler-Lagrange equation for the scalar field we can obtain the linear evolution equation for φ .

$$\varphi_{;\alpha}^{\alpha} + \delta\Gamma_{\alpha\beta}^{\beta} \phi^{;\alpha} + \Gamma_{\alpha\beta}^{\beta} \varphi^{;\alpha} + V''\varphi = f''\varphi \mathcal{L}_c + f'\delta\mathcal{L}_c \quad (49)$$

Perturbing the particle Lagrangian in (46)

$$\delta\mathcal{L}_a = -\delta m_a \delta(x - x_a(t)) (-g_{\mu\nu} \dot{x}^\mu \dot{x}^\nu)^{\frac{1}{2}} \quad (50)$$

and averaging over all dust particles, we have $\delta\mathcal{L} = -n \langle \delta m/u^0 \rangle = -\delta\rho_c$. The non-minimally coupled scalar perturbation equation becomes

$$\frac{\ddot{\varphi}}{a^2} + \frac{1}{2} \dot{h} \dot{\varphi} + 2 \frac{\dot{a}}{a} \dot{\varphi} + V''\varphi - \varphi_{;i}^i = -\rho_c (f''\varphi + f'\delta_c) \quad (51)$$

The perturbed Einstein equations can be used to obtain an expression for $\delta\rho$

$$(\rho + P)\theta + 3H(\delta\rho + \delta P) + \frac{1}{2}(\rho + P)\dot{h} + \dot{\delta\rho} = 0 \quad (52)$$

We are interested in the interacting dark matter and scalar field, which are not separable in (52)

$$\begin{aligned} f\rho_c\theta_c + 3H\delta(f\rho_c) + \frac{1}{2}(f\rho_c)\dot{h} + \frac{d}{d\tau}(\delta(f\rho_c)) \\ + \dot{\varphi} \frac{\nabla^2\varphi}{a^2} + 3H \left(\frac{2\dot{\varphi}\dot{\varphi}}{a^2} \right) + \frac{1}{2} \frac{\dot{\varphi}^2}{a^2} a^2 \dot{h} \\ + \left(\frac{\ddot{\varphi}\dot{\varphi}}{a^2} + \frac{\dot{\varphi}\ddot{\varphi}}{a^2} + 2 \frac{\dot{a}}{a} \frac{\dot{\varphi}\dot{\varphi}}{a^2} V'\varphi + V''\varphi\dot{\varphi} \right) = 0 \end{aligned} \quad (53)$$

Using the equations of motion for the background and perturbed scalar field we find that (53) simplifies substantially. Interestingly, we find that the coupling does not affect the first order dark matter perturbation equation

$$\dot{\delta}_c = -\theta_c - \frac{1}{2}\dot{h} \quad (54)$$

With the residual degree of freedom in the synchronous gauge we are free to fix one additional parameter, by convention we set $\theta_c = 0$ so that $\dot{\delta}_c = \frac{1}{2}\dot{h}$. Ignoring baryons, for simplicity, the second order perturbation equation becomes,

$$\begin{aligned} \ddot{\delta}_c + H\dot{\delta}_c + \frac{3H^2 f\Omega_c}{2} \delta_c = \\ -3H^2 \Omega_\gamma \delta_\gamma - 2\dot{\varphi}\dot{\varphi} + (a^2 V' - \frac{3H^2 \Omega_c f'}{2}) \varphi \end{aligned} \quad (55)$$

C. MAP error bar estimation

The standard error on the estimate of C_l , ΔC_l for an experiment with N frequency channels (denoted subscript n), each respectively with angular resolution $\theta_{n, fwhm}(\text{arcmin}) = \theta_n(\text{rad})/60 \times \pi/180$ and sensitivity σ_n per resolution element, scanning a fraction f_{sky} of the sky in bins of l size Δl is given by [47]

$$\Delta C_l \approx \left(\frac{2}{(2l+1)f_{sky}\Delta l} \right)^{0.5} [C_l + \bar{\omega}^{-1}\bar{\mathcal{B}}_l^{-2}]$$

$$\bar{\omega} \equiv \sum_n \omega_n, \quad \bar{\mathcal{B}}_l^2 \equiv \bar{\omega}^{-1} \sum_n \mathcal{B}_{nl}^2 \omega_n,$$

$$\omega_n \equiv (\sigma_n \theta_n)^{-2}, \quad \mathcal{B}_{nl}^2 \approx e^{-l(l+1)/l_s^2} \quad (56)$$

where we have assumed that the experimental beam is approximately Gaussian filtering scale $l_s \equiv \sqrt{8ln^2\theta_n^{-1}}$. We have assumed a useful sky fraction $f_{sky} = 0.65$ and $\Delta l = 50$, Table 1 shows the remaining parameters used, taken from [48].

TABLE I. MAP CMB Experimental Specifications

ν (GHz)	$\theta_{n, fwhm}$	$10^6\sigma$	N_{ch}
40	28'	8.2	4
60	21'	11.0	4
90	13'	18.3	8

The combined errors in Fig.9 are therefore $\Delta[C_l(\Lambda CDM) - C_l(NMC)] = \Delta C_l(\Lambda CDM) + \Delta C_l(NMC)$.

[1] S. Perlmutter et al, Ap. J. **483**, 565 (1997); S. Perlmutter et al (The Supernova Cosmology Project), Nature **391** 51 (1998).
[2] B.P. Schmidt, Ap. J. **507**, 46-63 (1998).
[3] A.G. Riess et al, Ap. J. **116**, 1009, (1998).
[4] M. Turner, M. White Phys. Rev. D **56** 4439, (1997)
[5] L Wang et al, ApJ. **530** 17 (2000)
[6] S. Perlmutter et al, Ap. J. **517**, 565 (1999)
[7] J.D. Barrow & F.J. Tipler, *The Anthropic Cosmological Principle*, Oxford UP, (1986), p. 668.
[8] C Wetterich, Nucl. Phys B. **302** 668 (1988)
[9] B. Ratra and J. Peebles, Phys. Rev D37 (1988) 321.
[10] J. Frieman, C. Hill, A. Stebbins, I. Waga, Phys. Rev. Lett, **75** 2077 (1995).
[11] P. Ferreira and M. Joyce, Phys.Rev.Lett. **79** (1997) 4740-4743.
[12] P. Ferreira and M. Joyce, Phys.Rev. D58 (1998) 023503.
[13] I. Zlatev, L. Wang, & P. Steinhardt, Phys. Rev. Lett. **82** 896-899 (1999).
[14] A. Albrecht & C. Skordis, Phys. Rev. Lett. **84**, 2076-2079 (2000).

[15] C. Skordis & A. Albrecht ,astro-ph/0012195
[16] J. Barrow, R. Bean, and J. Magueijo, MNRAS **316** L41 (2000)
[17] C. Armendariz-Picon, V. Mukhanov, Paul J. Steinhardt, astro-ph/0004134; astro-ph/0006373.
[18] R. Bean and J. Magueijo, astro-ph/0007199
[19] C. Brans and R. Dicke, Phys.Rev. 124 (1961) 925.
[20] F. Perrotta, C.Baccigalupi, S. Matarrese, Phys.Rev. D61 (2000) 023507.
[21] S. Carroll, Phys.Rev.Lett. 81 (1998) 3067-3070.
[22] Damour T., Polyakov A.M., Nucl.Phys. B423 (1994) 532-558; Gen.Rel.Grav. 26 (1994) 1171-1176.
[23] T. Damour, G. Gibbons, and C. Gundlach, Phys. Rev. Lett. 64 (1990) 123.
[24] L. Amendola, Phys.Rev. D60 (1999) 043501.
[25] J.P. Uzan, Phys.Rev. D59 (1999) 123510.
[26] A.A. Tseytlin and C. Vafa, Nucl.Phys. B372 (1992) 443-466; A. A. Tseytlin Class.Quant.Grav. 9 (1992) 979-1000.
[27] L. Amendola, astro-ph/9906073; astro-ph/9908023.
[28] Bean R., Hansen S., Melchiorri A. astro-ph/0104162
[29] Hamuy M. et. al., Astron J. **106** (1998) 2393
[30] Weller J. & Albrecht A., astro-ph/0106079
[31] C. Ma & E. Bertschinger, Ap. J. **455** 7 (1995)
[32] L.R. Abramo & F. Finelli astro-ph/0101014
[33] Seljak U., Zaldarriaga M, Ap. J. **469** (1996) 437-444
[34] E.F. Bunn, M. White, Ap. J. **480** (1997) 6-21
[35] Viana P., Liddle A. R., 1999, MNRAS, 303, 535.
[36] A.J.S. Hamilton & M. Tegmark, astro-ph/0008392
[37] H. Hoekstra, astro-ph/0102368
[38] C. Ma & E. Bertschinger, Ap.J.Lett. **484** (1997) L1-L5
[39] G. Efstathiou & J.R. Bond, MNRAS, astro-ph/9807103 (1998)
[40] G. Smoot et al., Ap. J. **386** L1 (1992), C. Bennett et al. ApJ **464** L1 (1996)
[41] S. Hanany et al., Ap.J.Lett., **545**, (2000) 5
[42] C.B. Netterfield et al., astro-ph/0104460
[43] N.W. Halverson et al., astro-ph/0104490
[44] M. Doran et al., astro-ph/0012139
[45] B.S. Mason et al., astro-ph/0101171
[46] P.J.E. Peebles "Principles of Physical Cosmology" (Princeton Series in Physics)
[47] J.R. Bond, G.Efstathiou, M. Tegmark MNRAS **291** L33 (1997)
[48] M. Tegmark et al. Ap. J. **530**, 133, (2000)